



OPEN Pathophysiological link between carotid atherosclerosis and cerebral white matter lesions

Wookjin Yang¹, Keun-Hwa Jung²✉, Kyung-Il Park^{2,3}, Matthew Chung², Jiyeon Ha², Eung-Joon Lee², Han-Yeong Jeong⁴, Jeong-Min Kim² & Seung-Hoon Lee²

Carotid atherosclerosis is associated with white matter hyperintensity (WMH), potentially resulting in cognitive and gait problems. We assessed the relationship between carotid atherosclerosis patterns and regional WMH, offering insights into possible mechanisms. We reviewed 1,058 consecutive healthy individuals in a health check-up program, who chose both optional carotid doppler ultrasonography and brain magnetic resonance imaging. Total, periventricular, and subcortical WMH volumes were measured using automatic segmentation and quantification. Carotid atherosclerosis stages were defined as: normal, no atherosclerosis; plaque without stenosis, atherosclerotic plaque without stenosis; anatomic stenosis, angiographic stenosis without sonographic flow alteration; and hemodynamic stenosis, sonography-measured hemodynamically significant stenosis. These stages were analyzed for association with regional WMH volumes using linear regression. Total and periventricular WMH volumes increased with anatomic and subsequent hemodynamic stenosis; however, only hemodynamic stenosis was independently associated with total (B [95% confidence interval], 0.240 [0.057–0.423]; $p = 0.010$) and periventricular WMH volumes (0.232 [0.066–0.399]; $p = 0.006$). Hemodynamic stenosis degree, not plaque extent and anatomic stenosis degree, was significantly associated with total (0.178 [0.033–0.323]; $p = 0.016$) and periventricular WMH volumes (0.176 [0.044–0.308]; $p = 0.009$). Subcortical WMH was not associated with carotid atherosclerosis. Hemodynamic compromise may be a key factor linking carotid atherosclerosis and WMH, mainly affecting periventricular white matter.

Since establishing its relationship with stroke¹, carotid atherosclerosis has been recognized and managed as one of the major treatable risk factors for stroke². In addition, the gradual advancement of carotid atherosclerosis may lead to alterations in the brain microstructure, including the development of white matter hyperintensity (WMH), which may result in other neurological issues such as cognitive impairment and gait disturbance^{3,4}. The association between carotid atherosclerosis and WMH has been documented over the years;^{5–10} however, the mechanism through which carotid atherosclerosis affects WMH remains unclear.

Recent concepts distinguishing mechanisms underlying regional WMH development may provide clues to explore the link between carotid atherosclerosis and WMH. Periventricular WMH may mainly result from small vessel hypoperfusion, while subcortical WMH may be influenced by complex mechanisms rather than hypoperfusion, including impaired glymphatic clearance function^{11–14}. The patterns of carotid atherosclerosis are highly variable; some patients exhibit profound atherosclerotic plaques without significant stenosis via positive arterial remodeling, whereas others may have hemodynamically severe stenosis. While the former have a higher overall atherosclerotic burden, the latter may be more prone to hypoperfusion in the brain. Thus, the white matter of patients with carotid atherosclerosis may be differently affected depending on the specific pattern of atherosclerosis.

In this study, we investigated the association between regional WMH volumes and various aspects of carotid atherosclerotic patterns, including the extent of atherosclerotic plaques, degree of anatomic and hemodynamic stenosis, and coexistence of intracranial atherosclerosis (ICAS). Thereby we aimed to explore how carotid atherosclerosis may be related to the development of WMH.

¹Department of Neurology, Asan Medical Center, Seoul, Korea. ²Department of Neurology, Seoul National University Hospital, Seoul National University College of Medicine, 101 Daehak-ro, Jongno-gu, Seoul 03080, Korea. ³Department of Neurology, Seoul National University Healthcare System Gangnam Center, Seoul, Korea. ⁴Department of Neurology, Seoul Metropolitan Government-Seoul National University Boramae Medical Center, Seoul, Korea. ✉email: jungkh@gmail.com

Methods

Study population

Seoul National University Hospital (SNUH) administers a health check-up program, allowing participants to choose optional diagnostic tests for various organs alongside the general health examination, based on personal preference. Between January 2015 and June 2021, data for consecutive individuals in the health check-up program at SNUH who opted for both carotid doppler ultrasonography (CDU) and brain magnetic resonance imaging (MRI) were retrospectively reviewed. The exclusion criteria were as follows: (1) significant structural abnormalities on initial fluid-attenuated inversion recovery (FLAIR) images that could affect the automatic segmentation process;¹⁵ (2) conditions interfering with CDU or magnetic resonance angiography (MRA) assessment; (3) non-atherosclerotic carotid stenosis; (4) history of carotid or intracranial revascularization; and (5) missing clinical information, ultrasonographic measurement data, or neck MRA scans. This study was conducted in accordance with the principles of the Declaration of Helsinki. The institutional review board at SNUH approved this study (No. H-2204-116-1317) and waived the need for informed consent because of the retrospective design.

Data collection and imaging parameters

Information on age, sex, hypertension, diabetes, hyperlipidemia, atrial fibrillation, chronic kidney disease, smoking, antithrombotic medication use, statin use, estimated glomerular filtration rate, hemoglobin A1c, low-density lipoprotein cholesterol, and high-sensitivity C-reactive protein were collected at the time of the index MRI. Chronic kidney disease was defined as an estimated glomerular filtration rate of <60 mL/min/1.73m². CDU was performed utilizing high-frequency linear transducers on LOGIQ E9 (GE), iU22 (Philips) or Affiniti 70G (Philips) ultrasound systems. Brain MRI was conducted using a 1.5T (Magnetom Espree, Siemens [$n=166$]; Signa HDxt, GE [$n=74$]; Achieva, Philips [$n=15$]; Ingenia, Philips [$n=4$]) or 3.0T (Discovery MR750W, GE [$n=515$]; Magnetom Skyra, Siemens [$n=196$]; Magnetom Verio, Siemens [$n=33$]; IngeniaCX, Philips [$n=19$]) MR scanner, employing protocols that included 3D T1-weighted (magnetization prepared rapid gradient echo, fast spoiled gradient echo, or turbo field echo), FLAIR, and intracranial/neck 3D time-of-flight (TOF) MRA sequences. The parameters employed in the MRI protocol are detailed in Table S1.

Carotid atherosclerosis patterns

Carotid atherosclerosis was assessed from three aspects based on CDU and neck MRA findings: carotid plaque extent, anatomic stenosis degree, and hemodynamic stenosis degree. Carotid atherosclerosis stages were then defined using these three indices. Detailed definitions of these indices are provided in the following sections and summarized in Tables S2–S3.

Carotid plaque extent

To assess the carotid plaque extent, 0 or 1 point was assigned to each of the common carotid arteries (CCAs) and proximal internal carotid arteries (ICAs) based on the presence of CDU-detected atherosclerotic plaques. The points were then totaled across the four vessel locations, resulting in a score ranging from 0 to 4 for each participant.

Anatomic stenosis degree

Using the reformatted maximal intensity projection images from the neck 3D-TOF MRA scans, the North American Symptomatic Carotid Endarterectomy Trial methods were employed to grade anatomic stenosis in both proximal ICAs. An experienced neurologist (WY, 11 years in neurology and stroke medicine) assessed anatomic stenosis degree, blinded to clinical and imaging data, scoring each side as: 0, no stenosis; 1, $<50\%$ stenosis; 2, 50–69% stenosis; 3, $\geq 70\%$ stenosis¹⁶. The higher score from both sides represented the anatomic stenosis degree on a 0–3 scale.

Hemodynamic stenosis degree

To evaluate hemodynamic stenosis, ICA peak systolic velocity (PSV), PSV ratio, and St. Mary's ratio measured by CDU were used. ICA PSV was measured at the highest velocity point. CCA PSV and end-diastolic velocity were measured in the distal CCA, within 2 cm below carotid bifurcation. The PSV ratio was calculated by dividing ICA PSV by CCA PSV. St. Mary's ratio was calculated by dividing ICA PSV by CCA end-diastolic velocity. Scores reflecting the hemodynamic stenosis severity were appointed to both proximal ICAs as follows: 0 (no stenosis), ICA PSV <125 cm/s, PSV ratio <2 , and St. Mary's ratio <8 ; 1 (50–69% stenosis), ICA PSV 125–230 cm/s, PSV ratio 2–4, or St. Mary's ratio 8–14; and 2 ($\geq 70\%$ stenosis), ICA PSV ≥ 230 cm/s, PSV ratio ≥ 4 , or St. Mary's ratio ≥ 14 ¹⁷. The hemodynamic stenosis degree for each participant was determined by selecting the higher score from both proximal ICA measurements on a 0–2 scale.

Carotid atherosclerosis stage

To rate the carotid atherosclerosis stage, we grouped the participants into four categories—normal, plaque without stenosis, anatomic stenosis, and hemodynamic stenosis—based on composite criteria involving carotid plaque extent, anatomic stenosis, and hemodynamic stenosis. The normal group included participants without atherosclerotic evidence in both CDU and MRA. Those with atherosclerotic plaque in CDU but without stenosis constituted plaque without stenosis group (i.e., carotid plaque extent score ≥ 1 , anatomic stenosis score 0, and hemodynamic stenosis score 0). Participants with angiographic carotid stenosis but without sonography-measured hemodynamically significant stenosis were placed into anatomic stenosis group (i.e., anatomic stenosis score ≥ 1 and hemodynamic stenosis score 0). Those with sonography-measured hemodynamically significant

stenosis were classified as hemodynamic stenosis group (i.e., anatomic stenosis score ≥ 1 and hemodynamic stenosis score ≥ 1).

Coexisting ICAS

The indices mentioned above primarily pertained to extracranial atherosclerosis (ECAS); nevertheless, atherosclerosis in the distal vasculature may also significantly impact WMH^{18–20}. Thus, we delineated categories indicative of concurrent ECAS and ICAS and assessed their associations with WMH volumes. Participants with any visually detectable stenosis in the distal ICA or M1/M2 segments of the middle cerebral artery on intracranial 3D TOF MRA, assessed using the Warfarin-Aspirin Symptomatic Intracranial Disease method²¹, were classified as having ICAS. Similarly, for this categorization, ECAS was defined as any visible stenosis in both CCAs or proximal ICAs on neck MRA. Subsequently, participants were classified into four groups: normal, ECAS only, ICAS only, and combined ECAS and ICAS.

Automatic white matter lesion volume quantification

WMH volumes on all MR images were automatically segmented and quantified by region using the Food and Drug Administration-cleared LesionQuant module of the NeuroQuant software (CorTechs Lab, San Diego, CA). Initially, FLAIR images from each patient were aligned and reconstructed using a 3D T1-weighted image. Then, the LesionQuant tool was employed to automatically segment and measure the elevated FLAIR signal intensity relative to the surrounding tissue intensity. Areas involving four or more voxels were defined as lesions. Based on their distribution, WMH lesions were categorized into periventricular lesions, defined as those touching the ventricle; leukocortical lesions, defined as lesions touching the grey matter; and deep lesions, defined as those encompassing all other supratentorial lesions²². In this study, we collectively considered leukocortical and deep lesions as subcortical lesions, based on their shared location in the subcortical areas and the lower need for distinguishing them in vascular diseases than in demyelinating diseases. The total WMH volume was calculated by adding the periventricular and subcortical WMH volumes. Segmentation data obtained from LesionQuant were visually examined to validate proper segmentation of WMH lesions without interference from artifacts. To account for individual variations in brain size, all WMH volumes were expressed as a percentage of each patient's intracranial volume.

Statistical analysis

Baseline continuous variables were compared using the Kruskal-Wallis test or Mann-Whitney U test, as appropriate. Categorical variables were compared using the chi-square test or Fisher's exact test, as appropriate. The Cochran-Armitage test and Jonckheere-Terpstra test were utilized to conduct trend analysis. Bivariate analyses using Pearson's correlation test or the Mann-Whitney U test were performed to examine potential associations between clinical variables and WMH volumes. We initially assessed the relationship between the four-category carotid atherosclerosis stage and regional WMH volumes, summarizing the differential effects of carotid atherosclerosis patterns on WMH. Subsequently, we conducted individual analyses for the scores representing various facets of carotid atherosclerosis (i.e., carotid plaque extent, anatomic stenosis degree, and hemodynamic stenosis degree) to examine their associations with WMH volumes. Linear regression analyses were employed to evaluate the aforementioned associations. For multivariable analyses, adjustments were made for age, sex, and variables with $p < 0.10$ in bivariate analyses with regional WMH volumes. Given the potential interference of ICAS with the association between carotid atherosclerosis and WMH, WMH volumes were compared between groups based on the presence of ECAS and ICAS. To accommodate the variability introduced by using different scanners for MRI scans, we conducted sensitivity analyses that incorporated MR scanner variables into the multivariable analyses. Two-sided probability values of < 0.05 were considered statistically significant. Statistical analyses were conducted using R version 4.2.2 (R Foundation).

Results

Among 1,167 consecutive participants underwent both brain MRI and CDU as part of the SNUH health check-up program, 1,058 were eligible for analysis according to prespecified patient inclusion criteria (Fig. 1 and Table S4). The median [interquartile range] age of the participants was 62 [56; 69] years, and 56.9% were men ($n = 602$). The baseline characteristics of the eligible population are described in Table 1.

In bivariate analyses, total and periventricular WMH volumes were potentially associated ($p < 0.10$) with age, hypertension, diabetes, hyperlipidemia, atrial fibrillation, smoking, antithrombotic drug use, statin use, hemoglobin A1c, and low-density lipoprotein cholesterol. The subcortical WMH volume showed potential associations with age, hypertension, smoking, and antithrombotic drug use (Tables S5 and S6). Distributions of scores representing the carotid plaque extent and anatomic/hemodynamic stenosis degrees are summarized in Table S7. Participants with more advanced carotid atherosclerosis were older and more frequently men with a higher prevalence of vascular risk factors and chronic kidney disease (Table 1). Total and periventricular WMH volumes began to increase with the emergence of anatomic stenosis and showed a significant increase with the advancement of hemodynamic stenosis. In the subsequent multivariable linear regression analysis, hemodynamic stenosis demonstrated an independent association with total (B [95% confidence interval], 0.240 [0.057–0.423]; β , 0.078; $p = 0.010$) and periventricular WMH volumes (0.232 [0.066–0.399]; 0.083; $p = 0.006$), whereas anatomic stenosis alone did not. The subcortical WMH volume remained unaffected by the carotid atherosclerosis stage (Fig. 2; Table 2). More advanced hemodynamic stenosis was significantly associated with the total (0.178 [0.033–0.323]; 0.072; $p = 0.016$) and periventricular WMH volume (0.176 [0.044–0.308]; 0.078; $p = 0.009$; Table 3). Meanwhile, the carotid plaque extent showed no association with WMH volumes (Table S8). The anatomic stenosis score showed some tendency to be associated with total WMH volume (0.048 [–0.009–

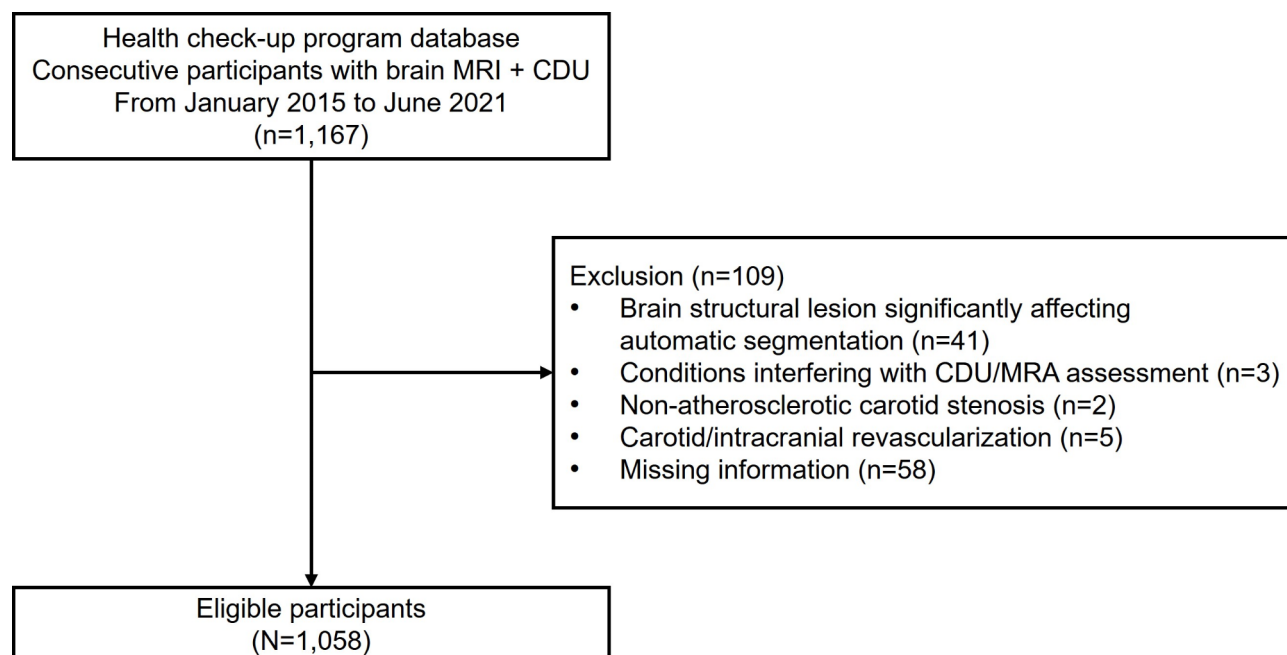


Fig. 1. Flowchart of participants inclusion and exclusion. CDU, carotid doppler ultrasonography; MRA, magnetic resonance angiography; MRI, magnetic resonance imaging.

	Total (n = 1,058)	Normal (n = 493) ^a	Plaque without stenosis (n = 418) ^a	Anatomic stenosis (n = 130) ^a	Hemodynamic stenosis (n = 17) ^a	p for trend
Age, years	62 [56; 69]	59 [53; 65]	64 [59; 71]	69 [61; 75]	74 [69; 78]	<0.001
Male sex	602 (56.9%)	250 (50.7%)	257 (61.5%)	84 (64.6%)	11 (64.7%)	<0.001
Hypertension	470 (44.4%)	167 (33.9%)	212 (50.7%)	77 (59.2%)	14 (82.4%)	<0.001
Diabetes	200 (18.9%)	64 (13.0%)	90 (21.5%)	41 (31.5%)	5 (29.4%)	<0.001
Hyperlipidemia	461 (43.6%)	176 (35.7%)	195 (46.7%)	79 (60.8%)	11 (64.7%)	<0.001
Atrial fibrillation	26 (2.5%)	8 (1.6%)	12 (2.9%)	5 (3.8%)	1 (5.9%)	0.059
Chronic kidney disease	42 (4.0%)	17 (3.4%)	15 (3.6%)	8 (6.2%)	2 (11.8%)	0.089
Ever smoking	472 (44.6%)	204 (41.4%)	197 (47.1%)	63 (48.5%)	8 (47.1%)	0.071
Antithrombotic drug use	250 (23.6%)	72 (14.6%)	108 (25.8%)	58 (44.6%)	12 (70.6%)	<0.001
Statin use	400 (37.8%)	146 (29.6%)	167 (40.0%)	75 (57.7%)	12 (70.6%)	<0.001
eGFR, mL/min/1.73m ²	85.0 [75.4; 93.6]	85.0 [75.4; 94.0]	86.3 [76.4; 93.9]	82.5 [74.0; 91.2]	77.5 [62.6; 98.1]	0.097
HbA1c, %	5.8 [5.5; 6.2]	5.7 [5.5; 6.0]	5.8 [5.5; 6.2]	5.9 [5.7; 6.6]	6.2 [5.9; 6.3]	<0.001
LDL cholesterol, mg/dL	115 [90; 140]	121 [93; 145]	112 [88; 137]	106.5 [80; 136]	92 [70; 111]	<0.001
hsCRP, mg/dL	0.0 [0.0; 0.1]	0.0 [0.0; 0.1]	0.1 [0.0; 0.1]	0.0 [0.0; 0.1]	0.0 [0.0; 0.1]	0.15

Table 1. Comparison of baseline characteristics according to the carotid atherosclerosis stage. Data are presented as No. (%) or median [interquartile range]. ^a Normal, individuals without evidence of atherosclerosis; plaque without stenosis, individuals with atherosclerotic plaque in carotid doppler ultrasonography but without stenosis; anatomic stenosis, individuals with angiographic stenosis but without sonography-measured hemodynamically significant stenosis; hemodynamic stenosis, sonography-measured hemodynamically significant stenosis. eGFR, estimated glomerular filtration rate; HbA1c, hemoglobin A1c; hsCRP, high-sensitivity C-reactive protein; LDL, low-density lipoprotein.

0.104]; 0.051; $p=0.099$; Table S9), however, this association was not statistically significant. No discernible association was found between any pattern of carotid atherosclerosis and subcortical WMH volume.

One hundred five participants had ICAS, with 60 having both ECAS and ICAS. Those with ICAS were characterized by older age; higher prevalence of hypertension, diabetes, hyperlipidemia, and chronic kidney disease; and more advanced carotid atherosclerosis. In particular, the group with both ECAS and ICAS had the highest proportion of participants with hemodynamic stenosis, followed by the ECAS-only group (Tables S10 and S11). Participants with isolated ECAS showed higher total and periventricular WMH volumes than did the control group; these differences were not seen for those with ICAS alone. Patients with both ECAS and ICAS

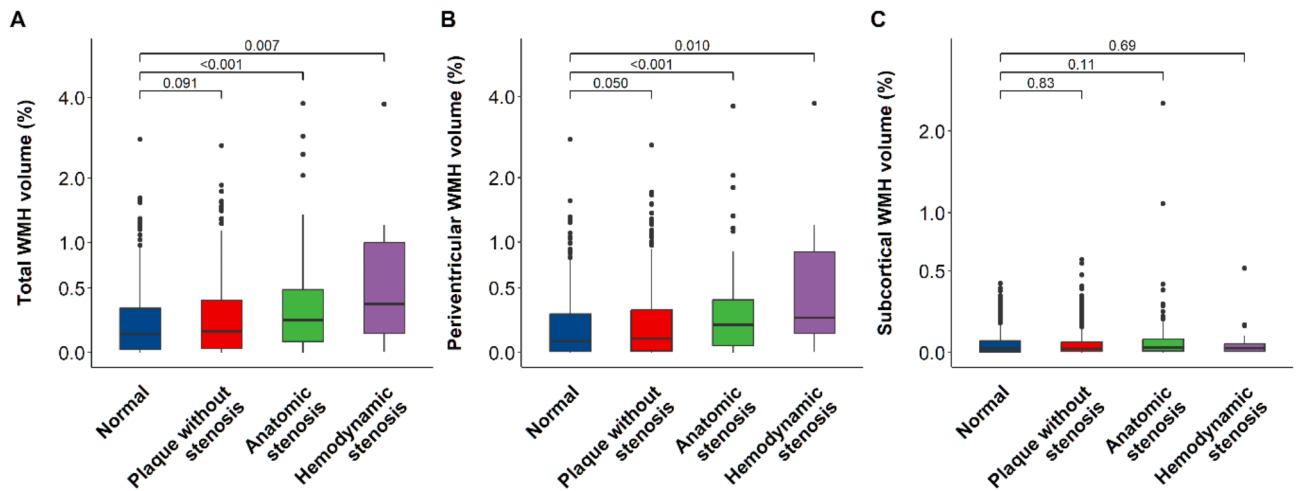


Fig. 2. Regional white matter hyperintensity volumes according to the carotid atherosclerosis stage. (A) Total, (B) periventricular, and (C) subcortical WMH volumes according to the carotid atherosclerosis stage. The WMH volumes are presented on the y-axis on a log scale. WMH, white matter hyperintensity.

	Total WMH volume			Periventricular WMH volume			Subcortical WMH volume		
	B (95% CI)	β	p value	B (95% CI)	β	p value	B (95% CI)	β	p value
Unadjusted									
Normal ^a	Reference			Reference			Reference		
Plaque without stenosis ^a	0.047 (-0.003-0.097)	0.060	0.063	0.044 (-0.001-0.089)	0.061	0.058	0.003 (-0.011-0.017)	0.015	0.65
Anatomic stenosis ^a	0.142 (0.068-0.216)	0.121	<0.001	0.114 (0.047-0.181)	0.107	<0.001	0.028 (0.007-0.049)	0.085	0.009
Hemodynamic stenosis ^a	0.412 (0.228-0.597)	0.134	<0.001	0.394 (0.226-0.562)	0.141	<0.001	0.018 (-0.034-0.071)	0.021	0.49
Age, sex-adjusted									
Normal ^a	Reference			Reference			Reference		
Plaque without stenosis ^a	-0.012 (-0.062-0.038)	-0.015	0.63	-0.012 (-0.058-0.033)	-0.017	0.60	0.000 (-0.015-0.015)	0.001	0.98
Anatomic stenosis ^a	0.041 (-0.034-0.116)	0.034	0.29	0.018 (-0.050-0.086)	0.017	0.60	0.022 (0.000-0.044)	0.068	0.047
Hemodynamic stenosis ^a	0.258 (0.077-0.439)	0.084	0.005	0.249 (0.084-0.414)	0.089	0.003	0.009 (-0.044-0.062)	0.011	0.74
Fully adjusted									
Normal ^a	Reference			Reference			Reference		
Plaque without stenosis ^a	-0.016 (-0.067-0.034) ^b	-0.021	0.52	-0.016 (-0.062-0.030) ^b	-0.022	0.50	-0.000 (-0.015-0.014) ^c	-0.002	0.96
Anatomic stenosis ^a	0.032 (-0.044-0.109) ^b	0.027	0.41	0.011 (-0.058-0.081) ^b	0.011	0.75	0.022 (-0.001-0.044) ^c	0.066	0.057
Hemodynamic stenosis ^a	0.240 (0.057-0.423) ^b	0.078	0.010	0.232 (0.066-0.399) ^b	0.083	0.006	0.007 (-0.047-0.061) ^c	0.008	0.79

Table 2. Linear regression analyses for associations between the carotid atherosclerosis stage and WMH volumes. ^a Normal, individuals without evidence of atherosclerosis; plaque without stenosis, individuals with atherosclerotic plaque in carotid doppler ultrasonography but without stenosis; anatomic stenosis, individuals with angiographic stenosis but without sonography-measured hemodynamically significant stenosis; hemodynamic stenosis, sonography-measured hemodynamically significant stenosis. ^b Adjusted for age, sex, hypertension, diabetes, hyperlipidemia, atrial fibrillation, smoking, antithrombotic drug use, statin use, hemoglobin A1c level, and low-density lipoprotein cholesterol level. ^c Adjusted for age, sex, hypertension, smoking, and antithrombotic drug use. B, unstandardized coefficient; β , standardized coefficient; CI, confidence interval; WMH, white matter hyperintensity.

	Total WMH volume			Periventricular WMH volume			Subcortical WMH volume		
	B (95% CI)	β	p value	B (95% CI)	β	p value	B (95% CI)	β	p value
Hemodynamic stenosis score ^a									
Unadjusted	0.285 (0.136–0.434)	0.115	<0.001	0.275 (0.139–0.410)	0.121	<0.001	0.010 (–0.032–0.052)	0.014	0.64
Age, sex-adjusted	0.192 (0.048–0.336)	0.077	0.009	0.189 (0.058–0.319)	0.084	0.005	0.003 (–0.039–0.046)	0.005	0.88
Fully adjusted	0.178 (0.033–0.323) ^b	0.072	0.016	0.176 (0.044–0.308) ^b	0.078	0.009	0.001 (–0.041–0.044) ^c	0.002	0.96

Table 3. Linear regression analyses for associations between the hemodynamic stenosis score and WMH volumes. ^a For the hemodynamic stenosis score, each proximal internal carotid artery was scored 0 to 2 based on ultrasonographic measurement as follows: 0 (no stenosis), ICA PSV < 125 cm/s, PSV ratio < 2, and St. Mary’s ratio < 8; 1 (50–69% stenosis), ICA PSV 125–230 cm/s, PSV ratio 2–4, or St. Mary’s ratio 8–14; and 2 (≥ 70% stenosis), ICA PSV ≥ 230 cm/s, PSV ratio ≥ 4, or St. Mary’s ratio ≥ 14. The higher score from both sides was selected. ^b Adjusted for age, sex, hypertension, diabetes, hyperlipidemia, atrial fibrillation, smoking, antithrombotic drug use, statin use, hemoglobin A1c level, and low-density lipoprotein cholesterol level. ^c Adjusted for age, sex, hypertension, smoking, antithrombotic drug use, and statin use. B, unstandardized coefficient; β , standardized coefficient; CI, confidence interval; WMH, white matter hyperintensity.

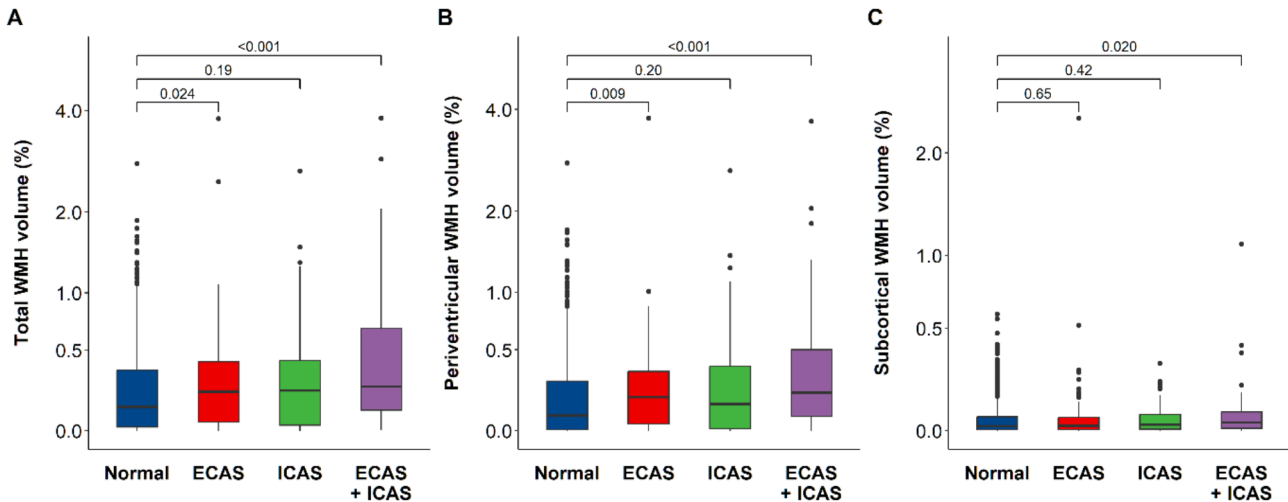


Fig. 3. Regional white matter hyperintensity volumes according to the presence of extra-/intracranial atherosclerosis. (A) Total, (B) periventricular, and (C) subcortical WMH volumes according to the presence of extra- and intracranial atherosclerosis. The WMH volumes are presented on the y-axis on a log scale. ECAS, extracranial atherosclerosis; ICAS, intracranial atherosclerosis; WMH, white matter hyperintensity.

showed the highest total, periventricular, and subcortical WMH volumes (Fig. 3). Although variations were noted in the distribution of WMH quantification data across MR scanners (Table S12), the differences in MR scanner did not impact the significance of our results (Table S13).

Discussion

Carotid atherosclerosis exhibited an association with WMH, primarily attributed to the advancement of hemodynamic stenosis rather than the carotid plaque extent and anatomic stenosis. The association between carotid atherosclerosis and WMH varied depending on the distribution of the hyperintensity, and there was a significant link with periventricular, but not subcortical, WMH. The effects of ECAS on total and periventricular WMH volumes were augmented by coexisting ICAS.

Several aspects of carotid atherosclerosis might influence cerebral white matter alterations. Vascular risk factors promoting carotid atherosclerosis, such as old age, hypertension, diabetes, and hyperlipidemia, may also contribute to WMH progression through pathways distinct from carotid atherosclerosis²³. Atherosclerosis-related artery-to-artery embolism may result in increased white matter lesions in individuals with high atherosclerotic burden¹⁰. Hemodynamically significant carotid stenosis may contribute to WMH development through compromised cerebral hemodynamics¹³. Our findings might imply that carotid atherosclerosis affect cerebral white matter through varying mechanisms at different stages, with hemodynamic factors playing a pivotal role. In the absence of hemodynamic compromise (i.e., plaque without stenosis and anatomic stenosis stages), individuals with carotid atherosclerosis may have higher WMH volumes, likely stemming from the effect of vascular risk factors on the vascular bed in the white matter, rather than the effect of the carotid

atherosclerosis itself. This is evidenced by attenuated associations with WMH volumes in these stages when assessed by multivariable linear regression analysis than by univariate comparison. In contrast, the independent association between hemodynamic stenosis and WMH volume implies a direct involvement of hemodynamic factors in linking carotid atherosclerosis and WMH. Thus, carotid atherosclerosis may exhibit a threshold relationship with WMH volumes, exerting a direct effect following the emergence of hemodynamic stenosis. The periventricular predominance observed in our study, consistent with the findings in previous reports^{24–27}, further supports the crucial role of hemodynamic factors in this association. Hemodynamic compromise in proximal carotid arteries may trigger downstream small vessel hypoperfusion, resulting in chronic ischemic injury in the small vessel border zone around the periventricular area and consequently increasing the periventricular WMH volume²⁸.

In our study, ICAS synergistically contributed to WMH in conjunction with ECAS, with the latter primarily driving this impact. Perhaps ECAS may have a broader hemodynamic effect on all downstream white matter regions, in contrast to the localized ischemic effects of ICAS. The notably elevated WMH volumes in participants with both ECAS and ICAS may imply that the presence of tandem lesions could further exacerbate chronic hypoperfusion in the periventricular area. The higher rate of hemodynamic stenosis in the group with both ECAS and ICAS may have influenced the results as well. However, the results of this analysis should be cautiously interpreted, because the categorization encompassing both ECAS and ICAS solely relied on anatomic stenosis criteria given the absence of hemodynamic data for ICAS.

The strength of this study was that it analyzed a large number of individuals with various stages of carotid atherosclerosis evidenced by CDU and MRA. Furthermore, the study employed fully automated segmentation and quantification of WMH volumes using Food and Drug Administration-cleared software. Compared to crude methods, including the Fazekas scale, this approach may reduce rater biases and enhance sensitivity for detection of even subtle white matter changes, particularly in healthy individuals like those in our health check-up program. However, this study also has several limitations. First, our database lacked data on hemodynamic measurements for ICAS and the collateral circulation. Access to hemodynamic data related to ICAS and collateral data could have influenced our analyses, possibly yielding other significant results. Second, this study lacks information on ultrasonography investigators over the period, hindering an evaluation of their impact on the results. Third, volumetric data by hemisphere could not be acquired using the LesionQuant software, and the analyses were conducted on a per-patient basis instead of a per-hemisphere basis. Thus, it was not possible to provide detailed information about the impact of vessel side on hemispheres, and different carotid artery sides may have been used for anatomic and hemodynamic stenosis analyses in some cases. Fourth, the retrospective, cross-sectional design of this single-center study limits generalizability and precludes establishing a causal relationship between advanced carotid atherosclerosis and WMH, necessitating future validation. Several key factors like medication adherence, lifestyle, and comorbidities (e.g., cardiac dysfunction) could not be controlled due to the retrospective design as well. The use of different imaging modalities for anatomical and hemodynamic stenosis may also have influenced the results. Finally, the small number of individuals in the hemodynamic stenosis group could have affected the statistical outcomes.

We suggested that hemodynamic compromise may be a key link in the relationship between carotid atherosclerosis and white matter changes, primarily affecting periventricular WMH. Periventricular WMH reportedly has a stronger association with adverse clinical outcomes, including cognitive impairment, than do subcortical lesions²⁹. Thus, pending verification through well-designed prospective longitudinal studies, patients with carotid atherosclerosis and progressive WMH might benefit from hemodynamic evaluation and carotid revascularization when indicated, as these interventions may potentially reverse white matter alterations³⁰. In addition, such serial changes in regional WMH volumes among patients with carotid atherosclerosis might potentially serve as predictive markers of future ischemic events.

Data availability

The data supporting the findings of this study are available from the corresponding author upon reasonable request.

Received: 10 July 2024; Accepted: 17 February 2025

Published online: 24 February 2025

References

1. Fisher, M. Occlusion of the internal carotid artery. *AMA Arch. Neurol. Psychiatry*. **65**, 346–377 (1951).
2. O. Kleindorfer, D. et al. Guideline for the prevention of stroke in patients with stroke and transient ischemic attack: A guideline from the American Heart Association/American Stroke Association. *Stroke* **52**, e364–e467 (2021). (2021).
3. DeBette, S. & Markus, H. S. The clinical importance of white matter hyperintensities on brain magnetic resonance imaging: Systematic review and meta-analysis. *BMJ* **341**, c3666 (2010).
4. Zheng, J. J., Delbaere, K., Close, J. C., Sachdev, P. S. & Lord, S. R. Impact of white matter lesions on physical functioning and fall risk in older people: A systematic review. *Stroke* **42**, 2086–2090 (2011).
5. Kwee, R. M. et al. Association between carotid plaque characteristics and cerebral white matter lesions: One-year follow-up study by MRI. *PLoS One*. **6**, e17070 (2011).
6. Avelar, W. M. et al. Asymptomatic carotid stenosis is associated with gray and white matter damage. *Int. J. Stroke*. **10**, 1197–1203 (2015).
7. Altaf, N. et al. Cerebral white matter hyperintense lesions are associated with unstable carotid plaques. *Eur. J. Vasc Endovasc Surg*. **31**, 8–13 (2006).
8. Ammirati, E. et al. Progression of brain white matter hyperintensities in asymptomatic patients with carotid atherosclerotic plaques and no indication for revascularization. *Atherosclerosis* **287**, 171–178 (2019).
9. Ammirati, E. et al. Relation between characteristics of carotid atherosclerotic plaques and brain white matter hyperintensities in asymptomatic patients. *Sci. Rep.* **7**, 10559 (2017).

10. Berman, S. E. et al. The relationship between carotid artery plaque stability and white matter ischemic injury. *Neuroimage Clin.* **9**, 216–222 (2015).
11. Jung, K. H. et al. Heterogeneity of cerebral white matter lesions and clinical correlates in older adults. *Stroke* **52**, 620–630 (2021).
12. Park, K. I. et al. Classification of white matter lesions and characteristics of small vessel disease markers. *Eur. Radiol.* **33**, 1143–1151 (2023).
13. ten Dam, V. H. et al. Decline in total cerebral blood flow is linked with increase in periventricular but not deep white matter hyperintensities. *Radiology* **243**, 198–203 (2007).
14. Huang, P. et al. Deep white matter hyperintensity is associated with the dilation of perivascular space. *J. Cereb. Blood Flow. Metab.* **41**, 2370–2380 (2021).
15. Yang, W. et al. Characteristics and clinical implication of white matter lesions in patients with adult moyamoya disease. *Neurology* **100**, e1912–e1921 (2023).
16. North American Symptomatic Carotid Endarterectomy Trial Collaborators. Beneficial effect of carotid endarterectomy in symptomatic patients with high-grade carotid stenosis. *N Engl. J. Med.* **325**, 445–453 (1991).
17. Oates, C. P. et al. Joint recommendations for reporting carotid ultrasound investigations in the United Kingdom. *Eur. J. Vasc. Endovasc. Surg.* **37**, 251–261 (2009).
18. Zhong, T. et al. Contribution of intracranial artery stenosis to white matter hyperintensities progression in elderly Chinese patients: A 3-year retrospective longitudinal study. *Front. Neurol.* **13**, 922320 (2022).
19. Feng, F. et al. White matter hyperintensities had a correlation with the cerebral perfusion level, but no correlation with the severity of large vessel stenosis in the anterior circulation. *Brain Behav.* **13**, e2932 (2023).
20. Lee, W. J. et al. Progression of cerebral white matter hyperintensities and the associated sonographic index. *Radiology* **284**, 824–833 (2017).
21. Samuels, O. B., Joseph, G. J., Lynn, M. J., Smith, H. A. & Chimowitz M. I. A standardized method for measuring intracranial arterial stenosis. *AJNR Am. J. Neuroradiol.* **21**, 643–646 (2000).
22. CorTechs Lab. *Defining and Classifying FLAIR lesions in LesionQuant* (2021). <https://www.cortechs.ai/defining-lesions>
23. Maillard, P., Carmichael, O. T., Reed, B., Mungas, D. & DeCarli, C. Cooccurrence of vascular risk factors and late-life white-matter integrity changes. *Neurobiol. Aging* **36**, 1670–1677 (2015).
24. Kandiah, N., Goh, O., Mak, E., Marmin, M. & Ng, A. Carotid stenosis: A risk factor for cerebral white-matter disease. *J. Stroke Cerebrovasc. Dis.* **23**, 136–139 (2014).
25. de Leeuw, F. E. et al. Carotid atherosclerosis and cerebral white matter lesions in a population based magnetic resonance imaging study. *J. Neurol.* **247**, 291–296 (2000).
26. Rimmele, D. L. et al. Association of carotid plaque and flow velocity with white matter integrity in a middle-aged to elderly population. *Neurology* **99**, e2699–e2707 (2022).
27. Ye, H. et al. White matter hyperintensities and their subtypes in patients with carotid artery stenosis: A systematic review and meta-analysis. *BMJ Open* **8**, e020830 (2018).
28. Smirnov, M., Destrieux, C. & Maldonado, I. L. Cerebral white matter vasculature: Still uncharted? *Brain* **144**, 3561–3575 (2021).
29. Ni, L. et al. Lower cerebrovascular reactivity contributed to white matter hyperintensity-related cognitive impairment: A resting-state functional MRI study. *J. Magn. Reson. Imaging* **53**, 703–711 (2021).
30. Yamada, K., Sakai, K., Owada, K., Mineura, K. & Nishimura, T. Cerebral white matter lesions may be partially reversible in patients with carotid artery stenosis. *AJNR Am. J. Neuroradiol.* **31**, 1350–1352 (2010).

Acknowledgements

None.

Author contributions

Conception and design: W.Y., K.-H.J., K.-I.P., M.C., J.H., E.-J.L., H.-Y.J., J.-M.K., and S.-H.L. Data acquisition: W.Y., K.-H.J., and K.-I.P. Data analysis and interpretation: W.Y. and K.-H.J. Drafting of the manuscript: W.Y. and K.-H.J. Revision of the manuscript: W.Y., K.-H.J., K.-I.P., M.C., J.H., E.-J.L., H.-Y.J., J.-M.K., and S.-H.L. Supervision: K.-H.J.

Funding

This study was supported by research grants from Chong Kun Dang pharmaceutical Corp (0620222380) and Ministry of Food and Drug Safety (RS-2023-00215667). The funding source had no role in study design, collection, analysis, and interpretation of data; in the writing of the manuscript; and in the decision to submit the manuscript for publication.

Declarations

Competing interests

The authors declare no competing interests.

Additional information

Supplementary Information The online version contains supplementary material available at <https://doi.org/10.1038/s41598-025-90922-3>.

Correspondence and requests for materials should be addressed to K.-H.J.

Reprints and permissions information is available at www.nature.com/reprints.

Publisher's note Springer Nature remains neutral with regard to jurisdictional claims in published maps and institutional affiliations.

Open Access This article is licensed under a Creative Commons Attribution-NonCommercial-NoDerivatives 4.0 International License, which permits any non-commercial use, sharing, distribution and reproduction in any medium or format, as long as you give appropriate credit to the original author(s) and the source, provide a link to the Creative Commons licence, and indicate if you modified the licensed material. You do not have permission under this licence to share adapted material derived from this article or parts of it. The images or other third party material in this article are included in the article's Creative Commons licence, unless indicated otherwise in a credit line to the material. If material is not included in the article's Creative Commons licence and your intended use is not permitted by statutory regulation or exceeds the permitted use, you will need to obtain permission directly from the copyright holder. To view a copy of this licence, visit <http://creativecommons.org/licenses/by-nc-nd/4.0/>.

© The Author(s) 2025